

Production of hypertritons in heavy ion collisions around the threshold of strangeness production

C. Hartnack¹, A. Le Fèvre², Y. Leifels² and J. Aichelin¹

¹ SUBATECH, UMR 6457, Ecole des Mines de Nantes, IN2P3/CNRS, Université de Nantes, 44307 Nantes, France

² GSI Helmholtzzentrum für Schwerionenforschung GmbH, Planckstraße 1, 64291 Darmstadt, Germany

Abstract

We use the Isospin Quantum Molecular Dynamics approach supplemented with a phase space coalescence to study the properties of the production of hypertritons. We see strong influences of the hyperon rescattering on the yields. The hypertritons show up to be quite aligned to the properties of nuclear matter underlining the necessity of rescattering to transport the hyperons to the spectator matter.

1. Introduction

The production of hypernuclei as extension of the common periodic system or as important ingredient for understanding strong interaction (see e.g. [1, 2, 3]) has recently gained strong interest for understanding the properties of the hyperon interaction with nuclear matter, in particular since the publication of recent results of experimental collaborations [4, 5, 6, 7]. Several theoretical approaches have proposed the combination of transport and fragmentation models in order to understand the data [8, 9, 10]. Very recently a novel fragmentation approach, FRIGA [11], based on the maximization of the binding energy of the fragments, succeeded in explaining FOPI data on hypertritons as well as brandnew data of HypHI [12] concerning hypertritons and $^4_{\Lambda}\text{H}$.

In this contribution we use a transport model, IQMD [13], supplemented by a phase space coalescence to study the properties of hypertritons in collision of Ni+Ni at an incident energy of 1.93 AGeV. This model shows quite comparable results for the hypertriton yields as the much more sophisticated analysis presented in [11].

2. Production of hyperons in heavy ion collisions

In this section we want only to sketch the production of hyperons in nuclear matter and refer for a detailed discussion to [14]. At energies around the threshold kaons are dominantly produced in multistep processes using resonances (especially the Δ) as intermediate energy storage. The energetically most favorable channel is the production of a kaon together with a hyperon, this channel being also the major channel for the hyperon production. This common production channel links the effects acting on the kaon production to that of the hyperon. Thus the hyperon yields are also depending on the nuclear equation of state and on the kaon optical potential: a soft EOS reaches higher densities than a hard one and thus causes a smaller mean free path of the nucleons which enhances the collision rate. This allows more deltas to undergo a second high energetic collision (and thus to produce a kaon-hyperon pair) before decaying again into a nucleon and a pion. However at these high densities the kaon optical potential causes a penalty on the strangeness production by enhancing the thresholds and thus lowering the production cross section for a given energy. This causes a reduction of the production of kaon-hyperon pairs with respect to calculations with a kaon optical potential.

This effect can be seen in Fig. 1 where we compare the spectra of K^0 and Λ measured by FOPI in collisions of Ni+Ni at 1.93 AGeV incident energy and IQMD calculations performed with (full line)

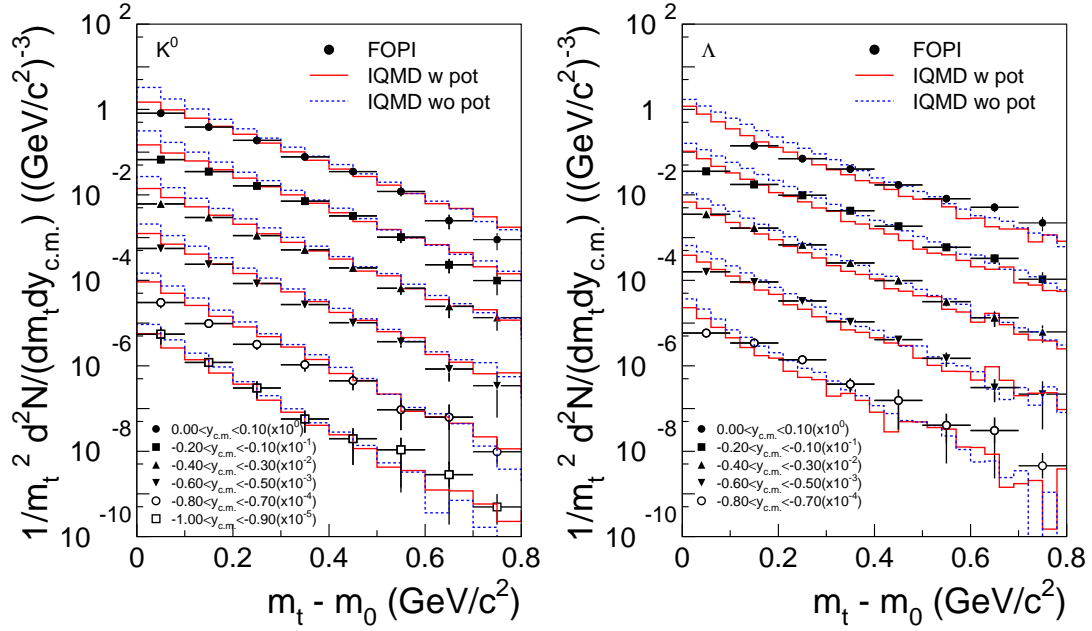


Fig. 1: Comparison of K^0 and hyperon spectra of Ni+Ni collisions between FOPI data and IQMD calculations

and without (dotted line) kaon optical potential. We see that the potential penalizes as well kaons as hyperons. The spectra are in good agreement, however it should be noted that the calculated temperatures for hyperons are somehow lower than the experimental values. It should also be noted that the rapidity distributions of the kaons measured by FOPI and KaoS can be well described.

Let us now compare the rapidity distributions of nucleons, hyperons and hypertritons. Fig.2 shows on the l.h.s the absolute yields as function of the rapidity. The ordinate is presented in logarithmic scale due to the large differences in absolute yields. This nicely demonstrates that the production of hypertritons is really a rare event. The r.h.s. shows the same distribution in linear scale but normalized to the particle yields. We see clearly that nucleons and hyperons are peaked in completely different regions in phase space. While the nucleon (dashed lines) peak around projectile and target rapidity, which means that the nuclear matter is not at all stopped, the hyperons (full line) peak around midrapidity. This is due to the effect that their production points are distributed around the cm of the colliding system which is typically the centre-of-mass of a NN system. It should be noted, that the production follows the kinematics of a 3 body phase space decay, where the hyperon has the highest mass - and thus the lowest velocity - of the 3 outgoing particles. Thus the hyperons show relatively low momenta at production in the NN centre of mass. The hypertritons (dotted line) have to combine Lambdas with nuclear spectator matter: their production peak lies in between the distributions of nucleons and hyperons but with a strong dominance of the nuclear matter.

3. The role of hyperon rescattering

The final rapidity distribution of the hyperons reflects not only the kinematics of the production process but also the rescattering with nuclear matter as it can be depicted from the l.h.s. of fig 3, where we

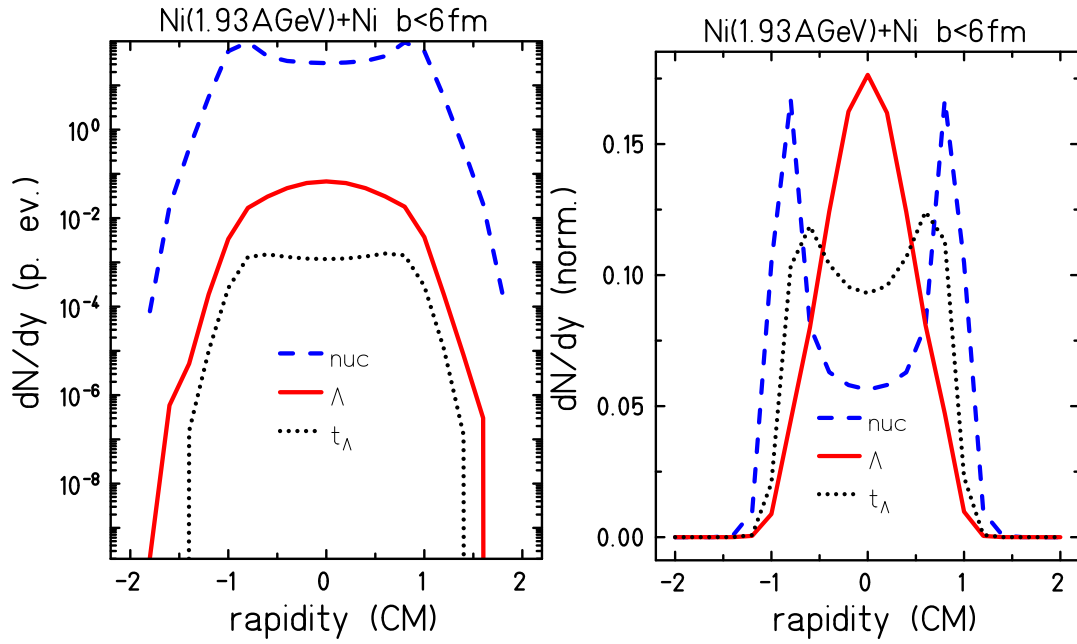


Fig. 2: Rapidity distributions of nucleons, hyperons and hypertritons in an absolute yield (left) and normalised to the total yield.

plot the normalized rapidity distributions of hyperons (full lines) and hypertritons (dotted lines). The rapidity distribution of hyperons with rescattering disabled (blue lines) correspond to the distribution at production and is therefore quite narrow. It is the rescattering (green thick lines) that enhances the momenta of the hyperons and thus leads to higher temperatures and broader rapidity distributions. This also influences the rapidity distributions of the hypertritons which need as well hyperons and nucleons for being created. The rapidity distribution of hypertritons is thus also broader if rescattering is allowed.

Besides the shape of the rapidity distributions of hypertritons, the rescattering influences also the yield of hypertritons significantly. This can be seen on the r.h.s. where the ratio hypertriton/hyperon is shown as function of the impact parameters using different options for the rescattering. The calculations using full rescattering (full lines) yield nearly 3 times more hypertritons than calculations disabling the rescattering (dash-dotted lines). If we set the rescattering cross sections to the half of its value (dotted lines) we still obtain nearly the double yield as in the calculations without rescattering. This can be easily understood from the rapidity distribution on the l.h.s. of fig 3: without rescattering the distribution of hyperons becomes this kind of narrow that only few hyperons can reach the region of spectator matter. However it is that region which is fertile for the production of fragments since it is there where clusters may remain undestroyed.

We can thus conclude that the main processus for creating hypertritons is to transport hyperons via rescattering to the region of the spectator matter where it may insert into a nucleon cluster. When having joined a cluster the hyperon-nucleon potentials help to keep the fragment stable. In this context we want to indicate that in IQMD the nucleons propagate by 2 and 3 body interactions of Skyrme, Yukawa, and Coulomb type, supplemented by momentum dependent interactions and asymetry potentials. Hyperons only interact by Skyrme interactions assuming a factor of two third in the strength of the potential. For details see [14].

The ratio of hypertritons/hyperons has the advantage to compensate other effects on the hypertriton yield stemming from the absolute hyperon yield. Effects acting on the kaon numbers like the equation

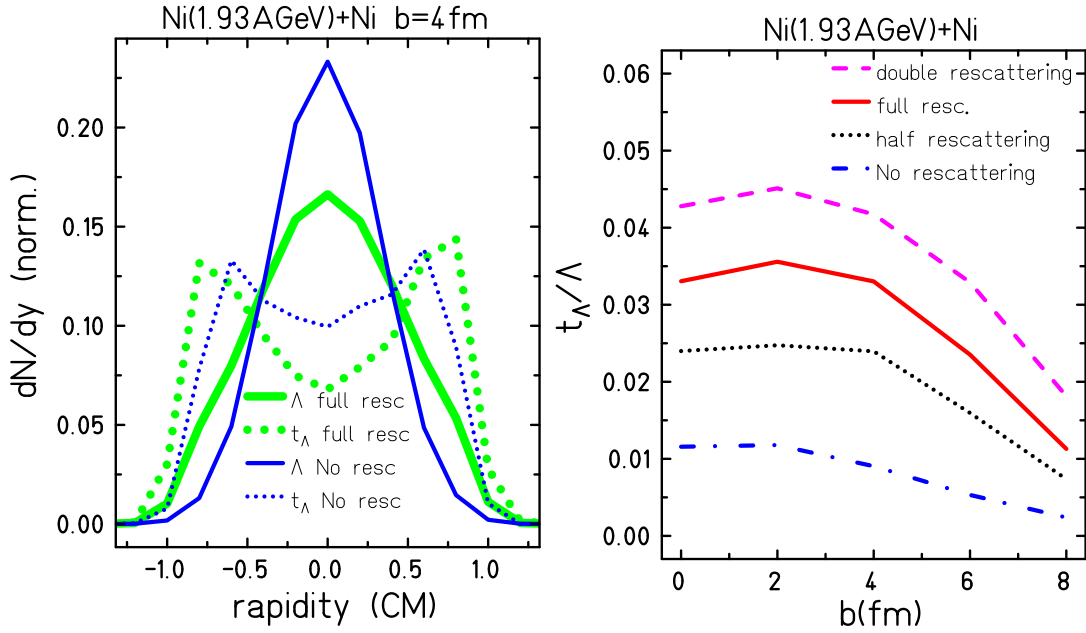


Fig. 3: Normalised rapidity distributions of hyperons and hypertritons with and without rescattering (left) and the ratio hypertritons/hyperons as a function of the impact parameter for different assumptions on the rescattering cross sections (right)

of state or kaon optical potentials of course influence the absolute yield of hypertritons.

Taking into account that the calculated hyperon spectra get lower temperatures than the experimental values we investigated the use of a novel cross section parametrisation inspired by ANKE data [15]. Fig.4 presents on the l.h.s. the “old” parametrisation (dashed line) and the new fit (full line) and on the r.h.s. its effect on the hypertriton to hyperon ratios as function of rapidity. We see that the enhanced cross sections also raise the ratios. For comparison we included results of a more sophisticated analysis [11] but which was still using the old parametrisation. That sophisticated analysis uses a minimum binding energies approach and applies the acceptance cuts of FOPI. We see a good agreement of our simplified model with these calculations which comforts us in using that simplified model for analysing the properties of hypertritons in detail.

4. Properties of hypernuclei

In order to show the correlation of hypertritons to nuclear matter let us compare the transverse flow of Lambdas (full line), nucleons (dashed line) and hypertritons (dotted line), shown on the l.h.s. of Fig. 5. We see that Lambdas show already a significant flow, which is dominantly due to the rescattering of the hyperons with the nuclear matter. That nuclear matter itself shows an even higher flow. Hypertritons show a flow compatible with the rest of the nuclear matter, which underlines the alignment of hypernuclei to the nuclear matter. It is due to a large number of collisions that the hyperons enters into the cluster.

This mechanism is supported by the observation of the freeze-out densities in the mid of Fig. 5: while the maximum density that a hyperon experienced (dashed line), typically the density of its production, is around twice time nuclear density, the freeze-out density (dotted line), i.e. the density of the last collisional contact, is quite lower. This indicates that the collisions persist up to a late phase of the expansion of the nuclear matter. If we regard the hyperons bound in a hypertriton (full line), they

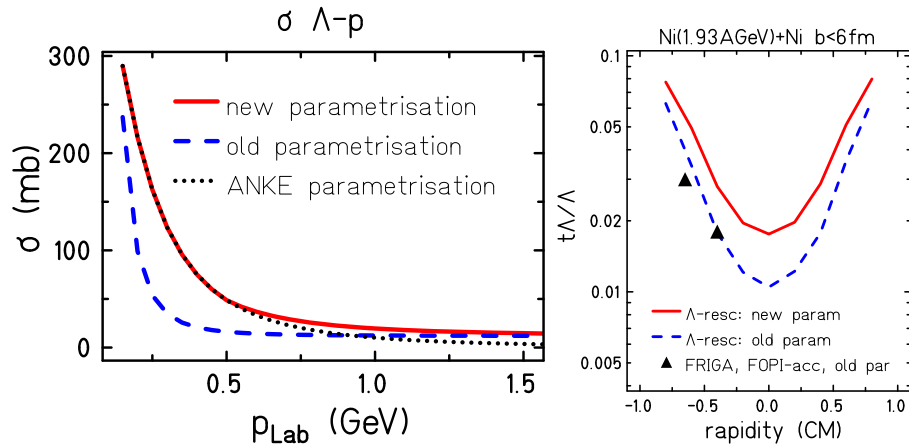


Fig. 4: Description of two parametrizations of rescattering and the hypertriton to hyperon ratio as function of rapidity.

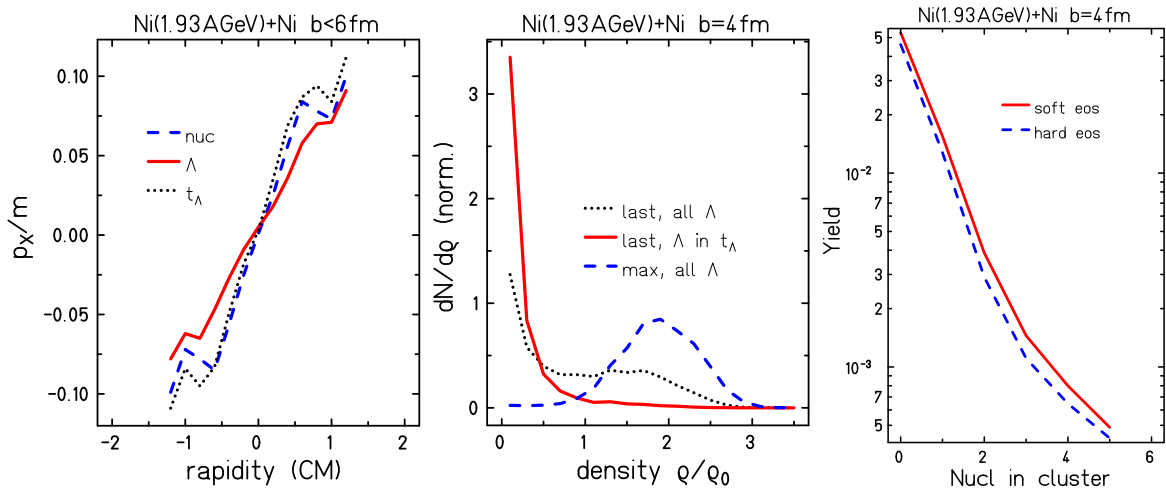


Fig. 5: Left: Transverse flow divided by the mass as function of the rapidity for Lambdas, nucleons and hypertritons. Mid: Maximum densities experienced by the Lambdas and densities at last contact for all Lambdas and Lambdas in hypertritons. Right: Yield of the clusters as a function of the numbers of nucleons in the cluster.

practically all freezed out at densities well below normal matter density.

Let us now look on the properties of hypernuclei at different cluster size. In the following we will describe the hypernuclei by the number of accompanying nucleons in the cluster. Zero means a single unclustered hyperon and serves to underline the difference between unclustered hyperons and hyperons in a cluster. As already indicated, the Lambda has to join the region of spectator matter in order to integrate a cluster. Since these regions are quite far away from the distributions of hyperons (see fig 2), their production is of course extremely suppressed. This finding is confirmed on the r.h.s. of fig 5, which describes the yield of the clusters as a function of the cluster size. The slight dependence of hypercluster yield on the nuclear equation of state is due to the effect of the EOS on the hyperon production. As already mentioned a soft EOS (full line) yields a higher hyperon yield than a hard EOS (dashed line) and thus more hyperclusters can be formed.

Let us first look on the dynamical observables of the clusters. Fig 6 shows on the l.h.s. the directed flow (normalised to the total mass) of the hyperclusters. As already seen on the l.h.s. of

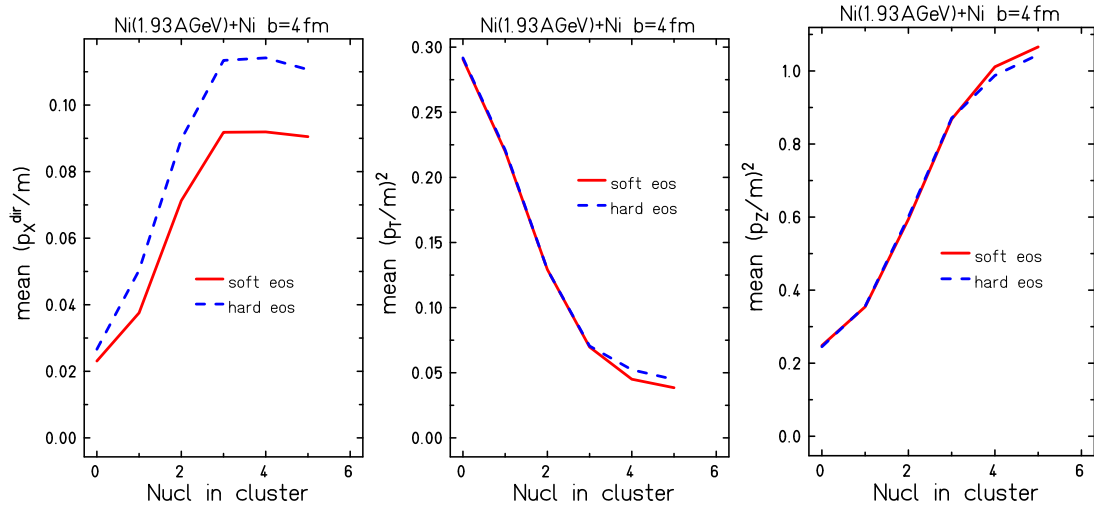


Fig. 6: Directed flow, mean quadratic transverse momentum and mean transverse longitudinal momentum of the hyperon as function of the cluster size

Fig. 5 even unclustered hyperons show a directed flow due to rescattering. Clustered hyperons show an enhanced flow, which increases with fragment size, an effect which is already known from the behaviour of normal nuclear fragments (“The fragments go with the flow”). At higher cluster sizes the flow value seems to saturate. It should also be noted that this observable shows a dependence on the nuclear equation of state, similar to the behaviour known for normal nuclear matter: a hard equation of state causes a higher directed flow.

The mid part and r.h.s. of Fig. 6 show respectively the squared transverse and longitudinal momenta, again normalised by the mass. The transverse momentum decreases with fragment size while the longitudinal momentum increases. This reflects the effect that large clusters can only be found at the projectile/target remnants which remain practically at projectile/target rapidities. This supports the previous statement that the production of large hyperclusters is strongly suppressed by the effect that only few hyperons enter the region of spectator matter.

5. Freeze-out of hypernuclei

As we have demonstrated in the previous section, the hyperons have to undergo rescattering in order to integrate a fragment. This effect is even more pronounced when going to larger hyperclusters. As already seen in the mid of fig 5 practically all hyperons found in a hypertriton show a very low freeze-out density. This feature remains for other hyperclusters as it can be depicted from the l.h.s. of fig 7, which presents the density (in units of the ground state density) at which the last collisional contact between the hyperon and the nuclear matter takes place. While unclustered hyperons freeze out at a density visibly higher than ground state density, while clustered hyperons freeze out at about on third of normal matter density.

The mid part of Fig. 7 presents the total number of collisions the hyperon has undergone in the reaction. Even if unclustered hyperons have already undergone almost 3 collisions with nucleons, the number of collisions increases strongly with the size of the cluster. In hypertritons the hyperons have already collided more than 7 times in the average. This means that many collisions are necessary in order to arrange the hyperon that way in nuclear matter that way that they can be bound into isotopes by the potentials.

The r.h.s. finally gives the “freeze-out time” of the hyperons, i.e the time when the last collision

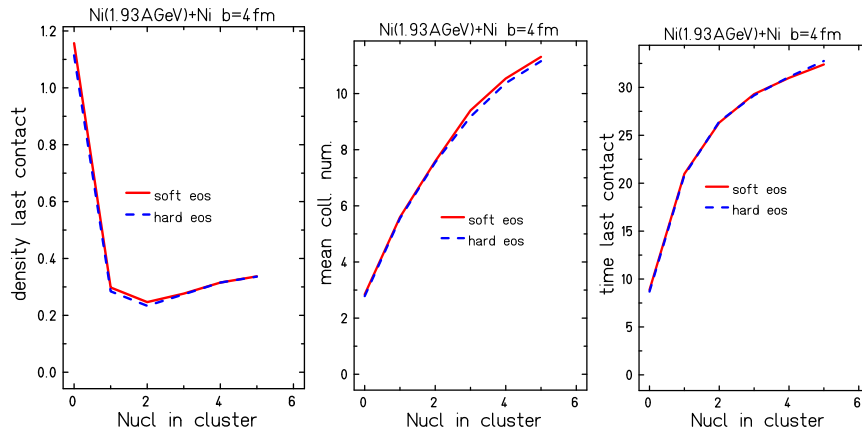


Fig. 7: Freeze-out density, mean collision number of the hyperon and freeze-out time of the hyperon as function of the cluster size

of a hyperon with a nucleon has happened. To give a reference point, the maximum density is reached after about 4-5 fm/c and the passing time (time which would be needed by the projectile to pass the target) is roughly 9 fm/c. This time corresponds exactly to the mean freeze-out time of unclustered nucleons. However, the formation of a hypertriton needs about 2-3 times the passing time and larger hyperclusters still stay in contact for more than 40 fm/c. This demonstrates again that a significant time of "rearrangement" is needed in order to allow a hyperon to take place in a cluster.

6. FRIGA results

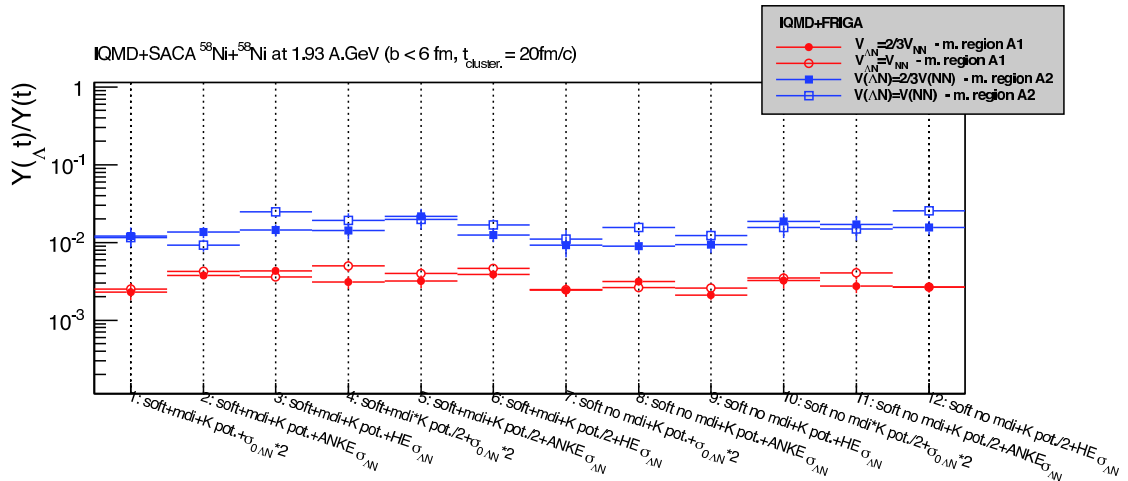


Fig. 8: FRIGA results on the ratio hypertriton/triton applying FOPI acceptance cuts

At the end of this article we want to summarize briefly several effects which can influence the absolute hypertriton yields. For this purpose we present on the r.h.s. of Fig. 8 the results of the FRIGA model on the ratio of hypertritons to tritons obtained in two different phase space regions accessible to FOPI. These phase space regions correspond to the rapidity marked by the triangles in Fig. 4. It should be note that experiment detects the hypernuclei by analysis of the vertex of the decay products ${}^3\text{He}$ and π^- (which have to be detected in a sufficiently large phase space region), by determination of

the invariant mass and by subtraction of combinatorical background. These constraints diminish the accessible region to two rather small areas.

FRIGA is a novel fragmentation approach described more in detail in [11]. It is working similarly to the SACA model [16] applying a Metropolis algorithm in order to find the configuration of maximum binding energy of the clusters. Like SACA it includes Skyrme type interactions and momentum dependent interactions but also surface and asymmetry energies. There is the additional possibility to include pairing energy and shell effects. In order to treat hypernuclei correctly FRIGA also includes hyperon-nucleons interactions, which are normally assumed to correspond to two third of the Skyrme potentials of nucleons. These results are presented in Fig. 8 by full symbols. Additionally calculations assuming the hyperon-nucleon interactions to be identical to the nucleon Skyrme interactions are presented by open symbols. We see that the second option changes the hypertriton yield slightly, since the binding of hyperons in nuclear matter is changed with the forces.

We see additionally the influence of the rescattering cross sections and the kaon optical potential. These results confirm the previous indications about the influence of these quantities: enhancing the cross sections enhances the hypertriton yields. Diminishing the kaon optical potential enhances also the hyperon yield and thus the number of hypertritons again. The preselection of parameters was restrained to calculations using a soft equation of state since the analysis of kaon data clearly indicates that the experimental data can only be explained by the use of a soft EOS [17, 18]. Preliminary results of the FOPI collaboration on this ratio exist, but still under reanalysis, thus an official release has not been published yet.

7. Conclusion

In conclusion we have demonstrated that the formation of hypertritons is strongly affected by the hyperon-nucleon rescattering, which allows the hyperons to enter the phase space of the clusters remaining from the spectator remnants. For that purpose a high number of rescattering is necessary. Hypernuclei show thus a low freeze-out density and a late freeze-out time. Their kinematical properties are strongly aligned to the behaviour of the spectator matter. Further analysis has to be done in order to allow for detailed comparison to nuclear data.

References

- [1] J. Schaffner, C.B. Dover, A. Gal, C. Greiner and H. Stöcker, *Phys. Rev. Lett.* **71**, 1328 (1993)
- [2] P. Papazoglou *et al.*, *Phys. Rev. C* **57**, 2576 (1998)
- [3] O. Hashimoto and H. Tamura, *Prog. Part. Nucl. Phys.* **57**, 564 (2006)
- [4] Y-G Ma (Star collaboration), EPJ Web Conf 66, 04020 (2014)
- [5] T.R. Saito *et al.* (HypHI collaboration), *Nucl. Phys. A* **881** (2012) 218
- [6] R. Lea, (Alice collaboration), *Nucl. Phys. A* **914**, 415 (2013)
- [7] Ch. Rappold *et al.* *Nucl. Phys. A* **913** (2013) 170
- [8] Th. Gaitanos, H. Lenske, U. Mosel, *Phys. Lett B* **675** (2009) 297
- [9] J. Steinheimer *et al.*, *Phys. Lett. B* **714** (2012) 85
- [10] A. Botvina, J. Steinheimer, E. Bratkovskaja, M. Bleicher, J. Pochodzalla, *Phys. Lett. B* **742** (2015) 7
- [11] A. Le Fèvre *et al.*, arXiv:1509.06648v1, to be published in J. Phys. G
- [12] Ch. Rappold *et al.*, *Phys. Lett. B* **747** (2015) 129.
- [13] C. Hartnack *et al.*, *Eur. Phys. J. A* **1**, 151 (1998)
- [14] C. Hartnack, H. Oeschler, Y. Leifels, E. L. Bratkovskaya and J. Aichelin, *Phys. Rep.* **510** (2012) 119
- [15] M. Büscher *et al.*, *Phys. Rev. C* **65**, 014603 (2002) [arXiv:nucl-ex/0107011].
- [16] P.B. Gossiaux, R. Puri, Ch. Hartnack, J. Aichelin, *Nucl. Phys. A* **619** (1997) 379-390.
- [17] C. Fuchs, A. Faessler, E. Zabrodin and Y. M. Zheng, *Phys. Rev. Lett.* **86**, 1974 (2001)
- [18] C. Hartnack, H. Oeschler and J. Aichelin, *Phys. Rev. Lett.* **96**, 012302 (2006) [arXiv:nucl-th/0506087].